JOURNAL OF MATERIALS SCIENCE 27 (1992) 592–598

High-temperature deformation of Al–Li–Cu–Mg–Zr alloys 8090 and 8091

XIA XIAOXIN*, J. W. MARTIN
Department of Metallurgy, Oxford University, Oxford OX1 3PH, UK

Specimens were prestretched in the range 0 to 7% plastic deformation prior to artificial ageing, or were duplex aged, to investigate the effect of dislocation substructure and of S(Al_2CuMg) particles on plastic flow during room and elevated temperature tensile tests. The yield stresses increased in Al–Li–Cu–Mg–Zr alloys 8090 and 8091 after stretching, due to the dislocation cells introduced by the stretch and also to the nucleation and growth of the S-phase particles on these dislocations. Up to 400 K the modulus-normalized proof stresses for the variously treated materials were constant, but they fell at higher temperatures, as dislocation climb mechanisms operated. The proof stresses of alloy 8090 fell at a temperature 50 K lower than alloy 8091, and this difference is considered to arise from the differing volume fraction of S-phase in the two alloys. The work hardening rate (ϑ) at a strain of 0.2% was measured between 300 and 500 K. In alloy 8090, the temperature at which dynamic recovery occurs was influenced by the degree of stretch, but this was not so in alloy 8091. In alloy 8090, the substructure introduced by stretching was able to act as a dislocation sink during dynamic recovery, whereas in alloy 8091 the higher copper content brought about more S-phase precipitation which was sufficient to inhibit this effect. The athermal hardening rate (ϑ_0) was obtained by extrapolation of the $\vartheta - \sigma_t$ curves, giving $\vartheta_0 = 10\,000$ GPa, for alloy 8090 and $\vartheta_0 = 8500$ GPa, for alloy 8091. This difference may reflect a higher mobile dislocation density in alloy 8090 due to the lower volume fraction of S-phase particles in that material.

1. Introduction

This work is concerned with two Al–Li–Cu–Mg–Zr alloys designated 8090 and 8091. The Young's modulus of these alloys is over 10% higher than that of other commercial aluminium alloys, and the main strengthening phase is the ordered δ' (Al_3Li) phase, which increases the strength by the formation of anti-phase boundaries during deformation. This leads to the movement of dislocation pairs during plastic deformation, and hence to planar slip [1]. Copper and magnesium are added to promote the formation of the semi-coherent S-phase (Al_2CuMg), which is heterogeneously nucleated. Precipitation of a high volume fraction of S-phase on dislocations will enhance the strength [2] as well as help to homogenize the co-planar slip distribution, and a more uniform distribution of S-phase particles is produced if the alloys are plastically deformed by stretch prior to ageing [3].

It has also been shown that the distribution of the S-phase may be made homogeneous by means of a duplex heat treatment introducing a period of natural ageing between solution heat treatment and artificial ageing [4]. The object of the present research is to study the effects of prior stretch and S-phase distribution upon the elevated temperature deformation behaviour of the alloys 8090 and 8091.

2. Experimental procedure

The alloys were in the form of rolled plates of 25 mm thickness, the chemical compositions (wt %) were as given in Table I. The alloys were thermomechanically processed as summarized in Table II. Cylindrical tensile specimens of gauge length 18 mm and diameter 5 mm were machined from the blanks after the various treatments, as shown in Fig. 1. The longitudinal axis was parallel to the rolling direction of the plate. The tensile tests were conducted over a range of temperatures between 300 and 550 K at a strain rate of $1 \times 10^{-3}\ s^{-1}$, the specimens being maintained in the furnace at test temperature for 0.5 h prior to testing.

3. Results

3.1. Microstructures

Transmission electron microscope (TEM) observations show that in the unstretched alloys 8090 and 8091, the S-phase particles primarily decorate the stray dislocations, grain and subgrain boundaries, as shown in Fig. 2. In duplex-aged 8090 and 8091, the S-phase distribution is more uniform, as shown in Fig. 3. This arises because the nature of the precipitation sites is influenced by the strong lithium to vacancy binding energy [4]. The homogeneous precipitation of S is

* *Present address*: Department of Metallurgy and Materials Engineering, Catholieke University, de Croylaan 2, B-3030, Leuven, Belgium.

0022–2461/92 $03.00 + .12

TABLE I The composition of alloys 8090 and 8091 (wt %)

Alloy	Li	Cu	Mg	Zr	Al
8090	2.41	1.16	0.61	0.11	Bal.
8091	2.40	2.00	0.70	0.15	Bal.

TABLE II Thermomechanical treatments applied. Specimen blanks of alloys 8090 and 8091 were solution-treated at 530 °C for 1 h, cold water quenched, then

No.	Treatment	Abbreviations	Ageing
1	Unstretched	N	Artificial 20 h, 190 °C
2*	2.5% stretched	2.5%	Artificial, 20 h, 190 °C
3	4% stretched	4%	Artificial, 20 h, 190 °C
4	7% stretched	7%	Artificial, 20 h, 190 °C
5	Duplex aged	D	Natural, 24 h, 21 °C, then Artificial, 24 h, 190 °C

*Alloy 8091 only.

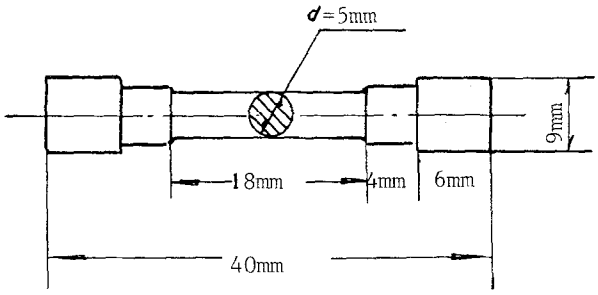

Figure 1 The tensile test specimen.

dependent on the density of free vacancies which, in turn, is a function of the solution treatment temperature and the temperature used for the first stage of the duplex age. During a low-temperature natural age, δ′ particles grow, and as they grow they incorporate lithium. The vacancies which were originally strongly bound to the lithium are released and can then condense to form nucleation sites for the S-phase during subsequent ageing. This model is supported by observations of the formation of dislocation loops and helices associated with δ′ growth [4], and by the direct observation of the nucleation of S at the δ′-matrix interface [5].

In stretched alloys 8090 and 8091, there is a uniform array of S-phase which is nucleated on the dislocations introduced by the stretch. A quantitative metallographic study of the S-phase distribution has shown [6] that in the stretched materials, the volume fraction and the size of the S-phase particles is higher than unstretched and duplex-aged materials. Fig. 4 shows TEM micrographs of the S-phase distribution in stretched 8090 and 8091.

3.2. Mechanical properties

3.2.1. Yielding behaviour

3.2.1.1. Alloy 8090. The duplex-aged, unstretched, 4% stretched and 7% stretched alloy 8090 tensile specimens were tested to fracture (between room temperature and 550 K). Load–extension curves for alloy 8090 at various temperatures are shown in Fig. 5, and the variation of the modulus-normalized 0.2% proof stresses ($\sigma_{0.2}/E$) against test temperature is shown in Fig. 6. For the duplex-aged, unstretched, 4% and 7% stretched samples, the 0.2% proof stress is constant up to 400 to 450 K. It is notable that the modulus-normalized proof stress of 4% stretched material is greater than that of the 7%, unstretched and duplex-aged materials.

All the proof stresses start to decline above 450 K, and at 550 K the proof stress of the 4% stretched alloy is greatest followed by the 7%, duplex-aged and unstretched materials.

3.2.1.2. Alloy 8091. The duplex-aged, unstretched, 2.5, 4 and 7% stretched alloy 8091 tensile specimens were also tested and load–extension curves for various temperatures are shown in Fig. 7. The relationship between the modulus-normalized 0.2% proof stresses and temperature is shown in Fig. 8, where it may be seen that alloy 8091 exhibits the same tendency as 8090. All the proof stresses remain constant, then fall above a critical temperature. Up to 400 K, the proof stress of 4% stretched 8091 samples are greater than those of the 7 and 2.5%, unstretched and duplex-aged materials, although there is rather less difference between them.

As the temperature increases, the yield stresses begin to fall at a temperature about 50 K higher than in alloy 8090. At 550 K, the 2.5% stretched alloy has the highest proof stress, followed by the 4 and 7%, unstretched and duplex-aged materials.

3.2.2. Work-hardening

3.2.2.1. Alloy 8090. The dynamic recovery behaviour of this alloy for various heat treatments and degrees of stretch have been studied by observing the change in work-hardening rate with temperature in the range 300 to 500 K. Fig. 5 shows that the slope ($d\sigma/d\varepsilon$) of the stress–strain curves decreases as the test temperature rises. This effect can be seen clearly when the modulus-normalized work-hardening rates (ϑ/E at 0.2% plastic strain), measured from load–extension curves by tangent construction, are plotted in Fig. 9. This figure shows an initially constant modulus-normalized work-hardening rate which then falls off as the temperature rises. The 7% stretched material is the first to show a decrease (at about 350 K), then the 4% stretched (at 400 K), unstretched (at 425 K), and duplex-aged materials follow (at 450 K). At low temperature, 7% stretched material shows the maximum work-hardening rate (ϑ/E), followed by the 4% stretched, unstretched and duplex aged materials. At 550 K, the work-hardening rate of the 7% stretched material remains the highest followed by the 4% stretched, duplex aged and unstretched materials in that order.

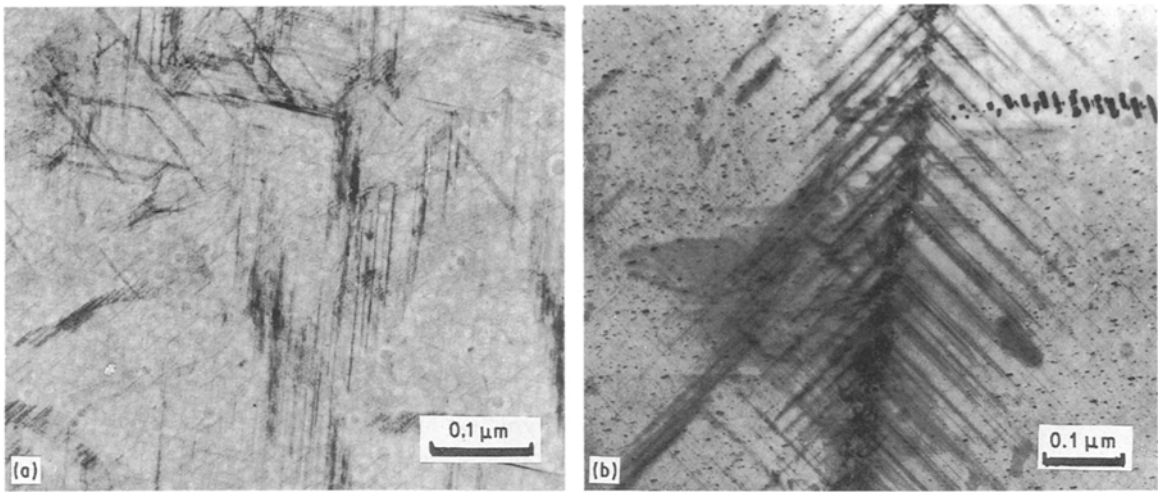

Figure 2 S-phase distribution in peak-aged unstretched alloys. (a) 8090, beam condition $(1\,1\,2)_{Al}$; (b) 8091, beam condition $(1\,0\,0)_{Al}$.

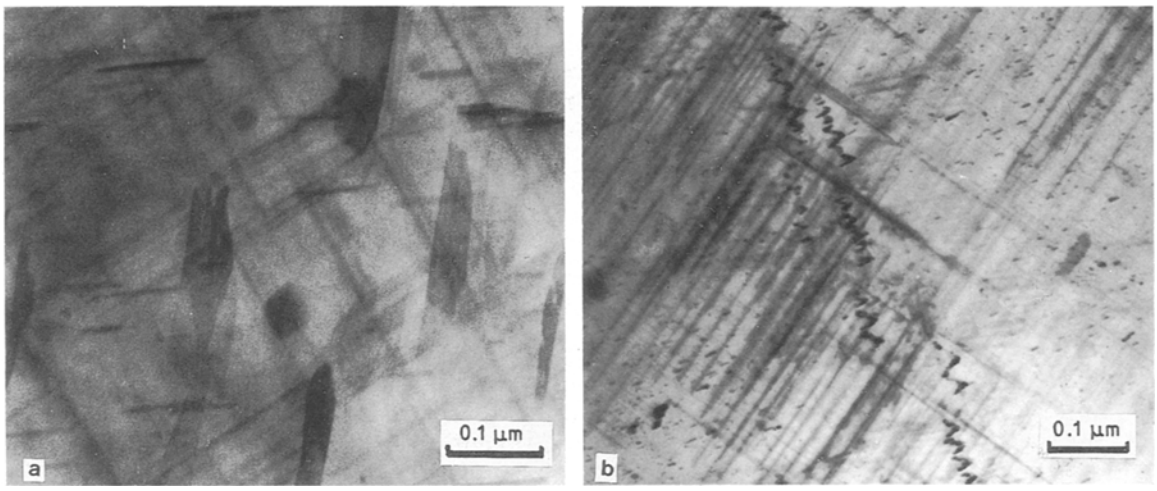

Figure 3 S-phase distribution in duplex-aged alloys. (a) 8090, beam condition $(1\,1\,2)_{Al}$, (b) 8091, beam condition $(1\,0\,0)_{Al}$).

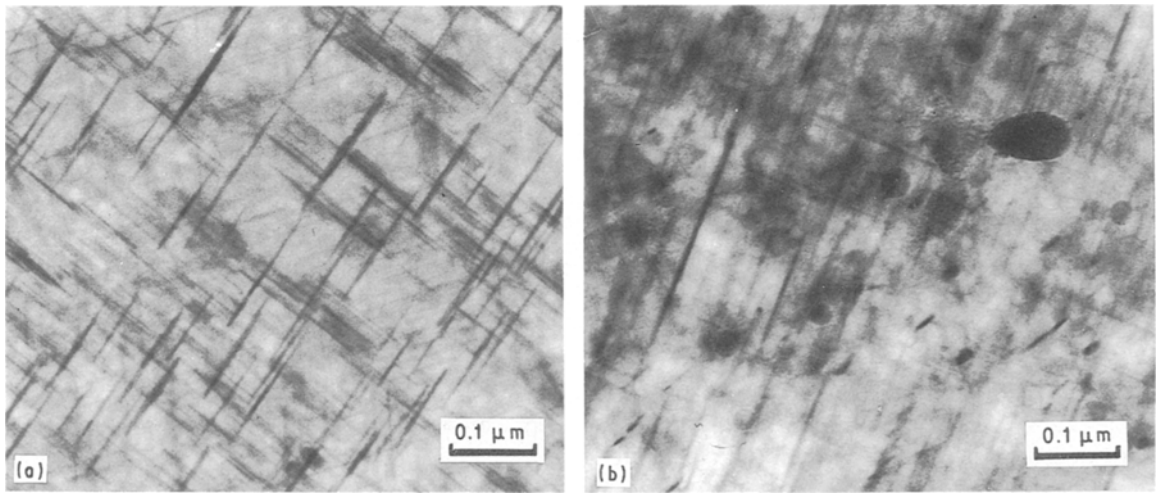

Figure 4 S-phase distribution in peak-aged 4% stretched alloys. (a) 8090, (b) 8091. beam condition $(1\,1\,2)_{Al}$.

3.2.2.2. Alloy 8091. The modulus-normalized work-hardening rates (ϑ/E) of alloy 8091 are plotted against test temperature in Fig. 10. In addition to using tangent construction, the values of work-hardening rate (ϑ) for alloy 8091 were obtained by using a computer to calculate the tangent from load–extension curves. The two methods produced identical results, confirming the accuracy of the procedure. The ϑ/E against test temperature curves of alloy 8091 show the same tendency as 8090, initially maintaining a constant level, but remaining constant to a higher temperature of about 450 K. Above this temperature, all the ϑ/E curves start to fall due to dynamic recovery, but the duplex-aged, unstretched and stretched materials do not differ much in dynamic recovery temperature, unlike alloy 8090.

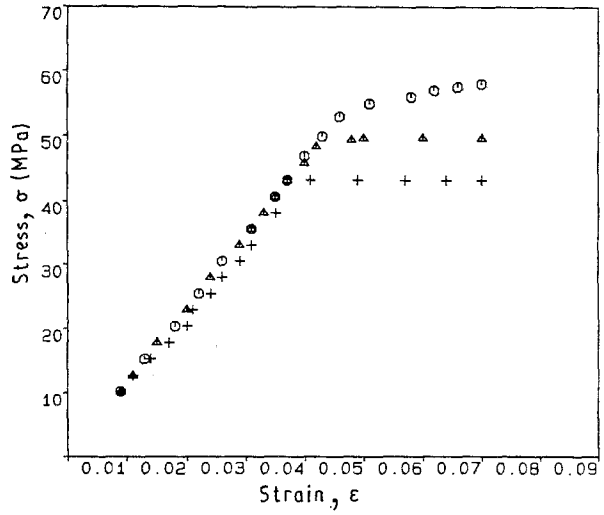

Figure 5 Load–extension curves for alloy 8090 at various temperatures: ○, 21; △, 177; +, 257 °C. 4% stretched.

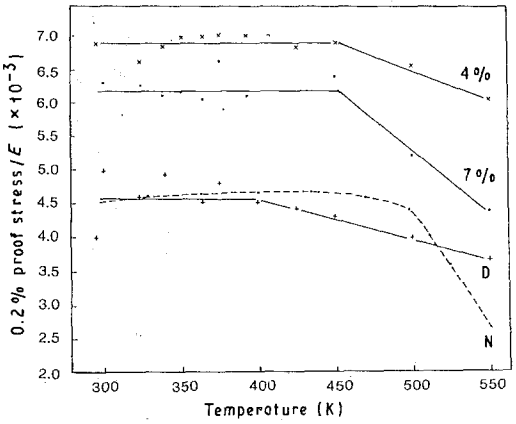

Figure 6 Variation of the modulus-normalized 0.2% proof stress with test temperature for alloy 8090. (– – –), from [3].

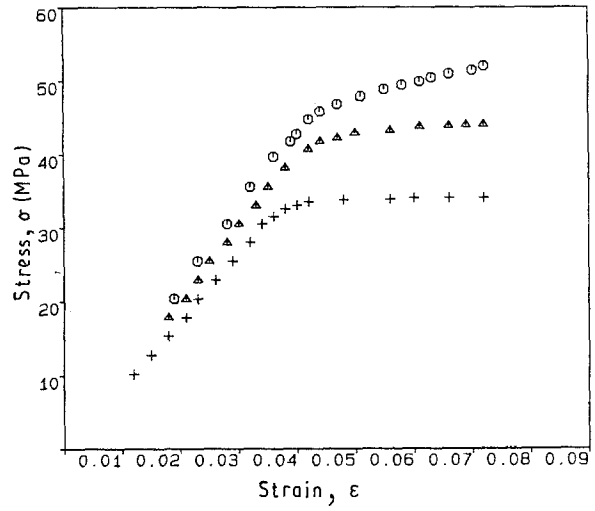

Figure 7 Load–extension curves for alloy 8091 at various temperatures: ○, 21; △, 177; +, 257 °C. 4% stretched.

3.3. Extrapolating data from the test curves

The work-hardening rate $\vartheta(d\sigma/d\varepsilon)$ at 0.2% plastic strain, and the work-hardening exponent n for alloys 8090 and 8091, were derived by computation from the experimental load–extension curves assuming an

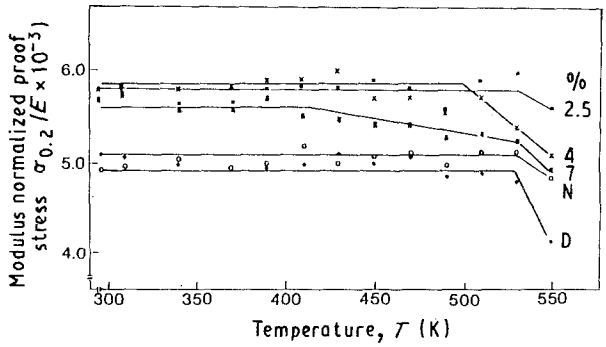

Figure 8 Variation of the modulus-normalized 0.2% proof stress with test temperature for alloy 8091.

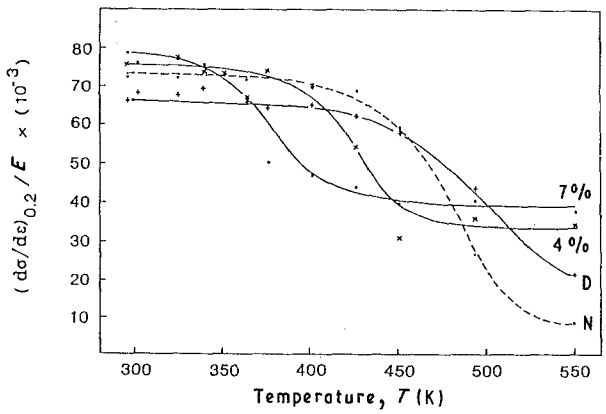

Figure 9 Variation of the modulus-normalized work hardening rate with test temperature for alloy 8090.

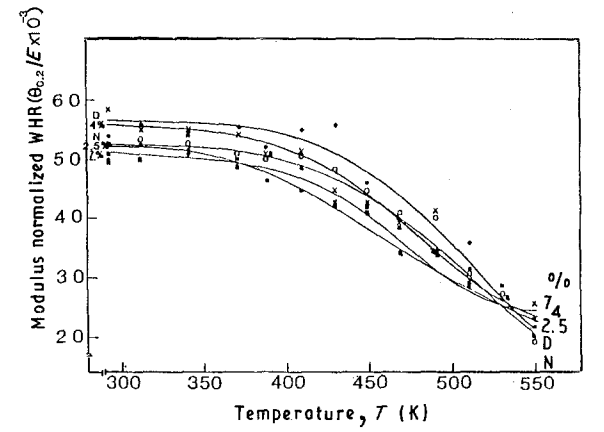

Figure 10 Variation of the modulus-normalized work hardening rate with test temperature for alloy 8091.

equation of the form $\sigma = A.\varepsilon^n$. The empirical Voce [8] equation

$$\vartheta = \vartheta_0(1 - \sigma_T/\sigma_0) \quad (1)$$

was applied to the data by plotting ϑ against the true stress (σ_T) (Figs 11 and 12), and thereby determining the athermal hardening rate ϑ_0 by extrapolation of the computed $\vartheta - \sigma_T$ curves.

In general, the data show a good linear relationship between ϑ and σ_T, with ϑ decreasing sharply with stress in all the test curves, and the higher the test

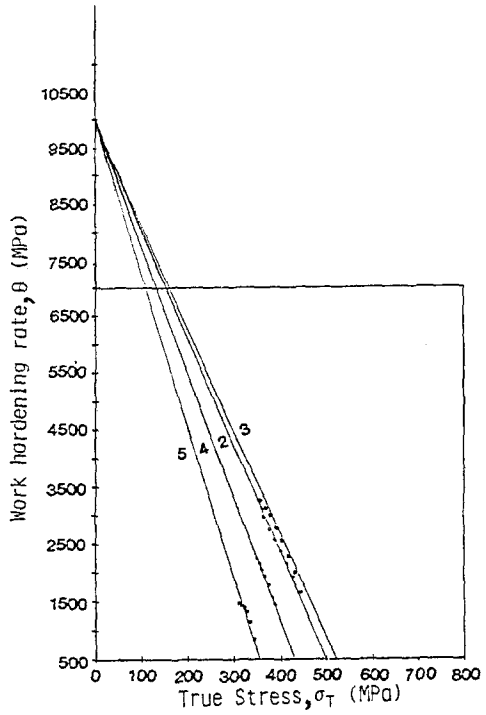

Figure 11 Voce plot for alloy 8090 (unstretched) at various temperatures.

No.	1	2	3	4	5
T (K)	323	373	406	440	470
σ_0	–	526	547	453	369

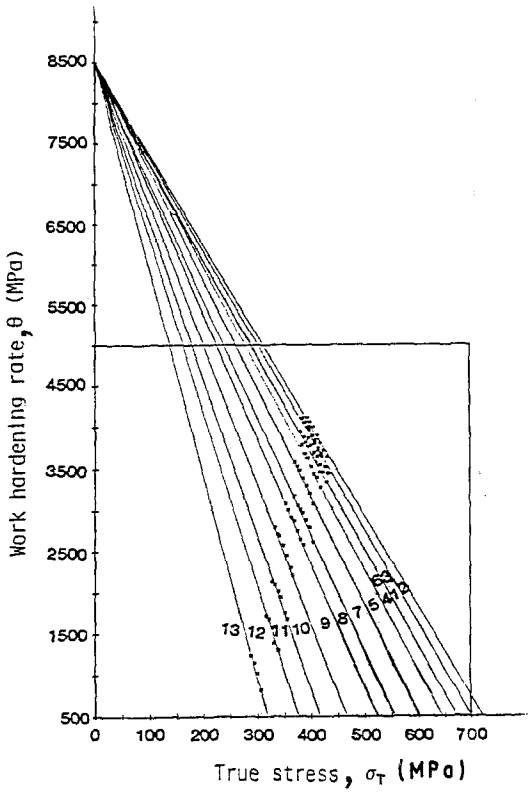

Figure 12 Voce plot for alloy 8091 at various temperatures.

No	1	2	3	4	5	6	7	8	9	10	11	12	13
T (K)	293	310	340	370	390	410	430	450	470	490	510	530	550
σ_0	749	771	749	712	680	712	638	590	553	499	446	404	340

temperature the steeper the curve. All the curves fit the Voce equation reasonably well.

4. Discussion

4.1. Yield behaviour

The contributions to the yield stress in Al–Li alloys come from various sources. Miller *et al.* [9] express them as follows

$$\tau_y = \tau_b + \tau_s + \tau_p \quad (2)$$

where τ_b is the contribution from grain, sub-grain boundary and dislocation substructure strengthening; τ_s is the contribution from solution strengthening; and τ_p the contribution from precipitation strengthening. τ_p in alloys 8090 and 8091 can be approximately written as

$$\tau_p = \tau_{\delta' sec} + \tau_S + \tau_{T1} \quad (3)$$

where τ_δ is the contribution from δ' phase; τ_S the contribution from S-phase; and τ_{T1} the contribution from T1 phase. Noble *et al.* [10] studied the contribution of solution strengthening, coherency strengthening, surface strengthening, order strengthening, stacking-fault and modulus strengthening, and concluded that in binary Al–Li alloys, order hardening and modulus hardening are important, but other contributions are negligible.

Flower and Gregson [5] studied the contribution of the T1 phase to the strength of Al–Li alloys, and concluded that the T1 phase is one of the main strengthening phases when co-precipitated with δ' and S-phase in Al–Li–Cu–Mg–Zr alloys, but that T1 is only important for strength when the copper content is greater than 3.5%, which is not the case with the 8090 and 8091 alloys.

TEM investigations show that for these aged materials, the variation of the stretch did not affect the size of the δ' phase, therefore the contribution to strength from the δ' phase should be considered as a constant for all the aged materials regardless of treatment. This conclusion is also reached by Cassada *et al.* [11].

The strength of the Al–Li–Cu–Mg–Zr alloys studies can thus be written as

$$\tau_y = \tau_b + \tau_S + \tau_{\delta'} \quad (4)$$

where $\tau_{\delta'}$ is a constant for all the peak aged materials. Thus the change in yield stress in these alloys is only related to changes in the dislocation substructure, and to the size and distribution of the S-phase particles.

We have shown that in Figs 6 and 7 the yield stresses increase after stretch. It is notable, however, that the 7% stretch results in a lower yield stress than the 4% stretched material in both alloys 8090 and 8091. This is due to the introduced dislocation substructure providing easy diffusion paths for copper and magnesium during artificial ageing. An increase in the S-phase particle size is observed, and these more widely spaced precipitates are less effective for particle strengthening, although the volume fraction in 7% stretched 8090 is higher than in the 4% stretched material, suggesting that the 7% stretched material is essentially overaged with respect to the S-phase distribution.

It is notable in Fig. 6 that the modulus-normalized yield stress of the duplex-aged 8090 decreases at a lower temperature than the unstretched material, due to the duplex-aged material containing a smaller size of S-phase particle. As the temperature rises, the dislocations are able to by-pass these particles more easily.

In alloy 8091, the proof stresses for various treatments begin to decrease at a higher temperature, which may be explained by the increased copper content in alloy 8091 giving rise to a higher volume fraction of S-phase particles.

4.2. Work-hardening behaviour.

The results suggest that at low temperatures, the dislocation substructure introduced by stretch provides a potent source of work-hardening for alloy 8090. This is not observed in alloy 8091 as its higher copper content will increase the volume fraction of S-phase precipitates in the grain, subgrain boundaries and dislocation substructures, immobilizing the dislocation sources.

4.2.1. Alloy 8090

The work-hardening rate values start to fall as the temperature rises, due to the glide dislocation finding sinks. TEM observations show that the plastic deformation (by stretch) results in dislocation cells which decrease in size with increasing degree of stretch, and the low volume fraction of S-phase particles in alloy 8090 is inadequate to immobilize all these dislocations. Thus the mean free path for dislocation recovery will be shortest in 7% stretched 8090, since the mobile dislocations can be readily absorbed by the dislocation cell walls in the dynamic recovery process. Material receiving the 4% stretch will have a larger cell size and a longer dislocation mean free path. It therefore has a higher critical softening temperature than the 7% stretched material. However the work-hardening rate of duplex-aged and unstretched materials begins to decrease at much higher temperatures than the stretched alloys, because of the absence of a dislocation cell structure to act as a sink to aid the onset of recovery. Only the grain and subgrain boundaries are available as dislocation sinks in the duplex-aged and unstretched alloys.

4.2.2. Alloy 8091

In Fig. 6, the work-hardening rate values from elevated-temperature tensile tests of alloy 8091 appear to be independent of the degree of prior stretch, in contrast to the behaviour of alloy 8090. This may be explained by the higher copper content in 8091, which increases the density of S-phase particles within the grain, subgrain, and dislocation substructures. It is suggested that these precipitates will prevent these regions from acting as a dislocation sink for dynamic recovery. Therefore the dynamic recovery behaviour in alloy 8091 is little affected by the various specimen conditions, and the work-hardening rate curves all show a decrease within a common narrow temperature range.

4.3. Comparison of experimental data and theoretical analysis

The conformity of the experimental data with the Voce equation is consistent with the dislocation models of dynamic recovery proposed by Kocks [12] and Kocks and Mecking [13]. It is striking that a single value for the extrapolated athermal hardening rate is observed for each alloy, independent of its thermomechanical treatment. The lower athermal hardening rate in alloy 8091 may arise from the greater volume fraction of S-phase in that alloy. This phase precipitates on the dislocations, and thus may more effectively lock the dislocation sources than is possible in 8090.

5. Conclusions

1. The variation of yield stress with temperature in alloys 8090 and 8091 mainly arises from the S-phase and the dislocation substructures introduced by the stretch.

2. At low temperature, the 4% stretched material shows the highest modulus-normalized proof stress among the stretched, unstretched and the duplex-aged materials, which implies a particle-size effect from the S-phase distribution in that material.

3. The values of the proof stresses drop as the temperature rises, due to the deformation mechanism changing from one of dislocation glide to one of climb.

4. The proof stress of alloy 8091 decreases at a temperature 50 K higher than that of alloy 8090, as the higher Cu content in 8091 brings about a higher volume fraction of S-phase particles. These S-phase particles hinder the dislocation climb at yield.

5. In the peak-aged condition, in alloy 8090 the grain, subgrain boundaries and dislocation cells introduced by stretch act as dislocation sinks during dynamic recovery. The mechanism by which this occurs is believed to be mainly by the dislocation cell walls incorporating or annihilating glide dislocations as they enter the substructure.

6. A high degree of stretch in alloy 8090 decreases the temperature at which dynamic recovery occurs. This is because a smaller substructure size forms after the stretch, which increases the dislocation sink density.

7. Alloy 8091 contains more S-phase and T1 phase particles on the grain, subgrain and dislocation substructures. The work-hardening rate values are maintained to higher temperature than in alloy 8090. The extra S-phase and T1 phase particles appear to 'lock' the dislocations and so hinder dynamic recovery.

8. The athermal hardening rate is a material-dependent parameter which has a higher value for alloy 8090 than 8091. This may reflect the higher density of mobile dislocations in 8090. The test results and analysis show that for Al–Li–Cu–Mg–Zr alloys 8090 and 8091, the relation of work-hardening rate and true stress is linear, in accord with the Voce equation.

Acknowledgements

The authors are grateful to Professor Sir P. B. Hirsch FRS for the laboratory facilities made available, and to R. A. E. Farnborough for the supply of materials. X. Xia gratefully acknowledges the support of the Lee Hysan Foundation of St. Hilda's College, Oxford, and of a British ORS Award.

References

1. J. W. MARTIN, "Micromechanisms in Particle-hardened Alloys" (Cambridge University Press, London, 1980).
2. P. J. GREGSON, K. DINSDALE, S. J. HARRIS and B. NOBLE. *Mater. Sci. Tech.* **3** (1987) 7.
3. P. J. E. BISCHLER and J. W. MARTIN, in "Al Technology 86" edited by T. Sheppard, (Institute of Metals, London, 1986) p. 442.
4. H. M. FLOWER, P. J. GREGSON, C. N. J. TITE and A. MUKHOPADHYAY, in Proceedings of an International Conference on Al–Li Alloys, their Physical and Mechanical Properties, Charlottesville, Virginia, USA, June 1986, edited by T. H. Sanders Jr. and E. A. Starke Jr. (Eng. Mat. Advisory Service, Warley, 1986) Vol II, p. 743.
5. H. M. FLOWER and P. J. GREGSON, *Mater. Sci. Tech.* **3** (1987) 81.
6. V. RADMILOVIC, G. THOMAS, G. J. SHIFLET and E. A. STARKE, Jr., *Scripta Met.* **23** (1989) 1141.
7. X. XIA and J. W. MARTIN, *Mater. Sci. Engng* **A128** (1990) 113.
8. E. VOCE, *J. Inst. Metals* **74** (1948) 537.
9. W. S. MILLER, J. WHITE and D. J. LLOYD, *J. Phys. Coll.* **C3** (1987) 139.
10. B. NOBLE, S. J. HARRIS and K. DINSDALE, *J. Mater. Sci.* **17** (1982) 461.
11. W. A. CASSADA, G. J. SHIFLET and E. A. STARKE Jr., *J. Phys. Coll.* **C3** (1987) 397.
12. U. F. KOCKS, in "Deformation Processing and Structure" edited by G. Krauss (ASM, Metals Park, Ohio, 1982).
13. U. F. KOCKS and H. MECKING, in Proceedings of the 5th International Conference Strength of Metals and Alloys, Aachen, 1979, edited by P. Haasen et al., (Pergamon Press, Oxford, 1979). Vol 1, p. 345.

Received 26 March
and accepted 20 December 1990